H∞ Design of an EM-ΣΔ Feedback for MEMS Gyroscopes

F. Saggin, Anton Korniienko, G. Papin, E. Markiewicz, Y. David, A. El Hajj, Gérard Scorletti

H_∞ Design of an EM-ΣΔ Feedback for MEMS Gyroscopes

F. Saggin[1], A. Korniienko[1], G. Papin[2], E. Markiewicz[1], Y. David[2], A. El Hajj[1], G. Scorletti[1]

[1] Laboratoire Ampère (UMR5005), Ecole Centrale de Lyon
36 av. Guy de Collongue
69134 Écully
FRANCE

[2] Tronic's Microsystems SA,
98 rue du Pré de l'Horme
38926 Crolles
FRANCE

Inertial Sensors and Systems 2020
Braunschweig, Germany

978-1-7281-6848-7/20/$31.00©2020 IEEE

Abstract

In this work, we propose a systematic and flexible method for designing the electronic filter of electro-mechanical ΣΔ (EM-ΣΔ) feedbacks, widely used for the closed-loop operation of high-performance MEMS gyroscopes. We formulate the filter design as an optimization problem based on the H_∞ norm of weighted closed-loop transfer functions with an appropriate H_∞ criterion. The desired closed-loop system specifications are then expressed through weighting filters, which can be chosen by the system designer. Practical implementations demonstrate the effectiveness of our method. When compared to the results of an established filter, we obtain performance improvements of 30% for the scale factor nonlinearity, 40% for the RMS noise, 35% for the angle-random walk, to cite a few.

1. Introduction

MEMS gyroscopes are micromachined devices widely employed to measure the rotation of objects. Their main features are easy integration in electronic devices, low cost, and low power consumption. However, MEMS sensors have a degraded precision when compared to other technologies. Therefore, in the last decades, efforts have been devoted to improve the performance of MEMS gyroscopes through the use of control loops.

MEMS gyroscopes are composed of two orthogonal oscillating modes: the drive and sense modes. Controlled oscillations are sustained on the drive mode, such that, when the sensor is submitted to an angular rate Ω_z, a Coriolis force appears, transferring part of the oscillation energy to the sense mode. The Coriolis force is proportional to Ω_z; then, by detecting the oscillations along with the sense mode, the Coriolis force and the angular rate can be computed.

In this work, we focus on the closed-loop operation of the sense mode, also known as force-to-rebalance loop. The main objective of this approach is to use a controller that, through the actuation circuit, applies a force on the sense mode that compensates for the Coriolis one. To this purpose, the well-known electro-mechanical ΣΔ (EM-ΣΔ) architecture has been widely employed [1-6]. We can mention three main benefits of this approach. First, like other closed-loop strategies, the bandwidth, linearity, dynamic range, and robustness of the sensor are improved. Second, the use of a relay (1-bit quantizer) for the actuation avoids problems linked to the nonlinear relationship between voltage and force of electrostatic actuators, improving the linear behavior of the device. Finally, being the output signal coded into a single bit, the interface with the digital processing circuits is straightforward.

The EM-ΣΔ architecture is inspired by the classical ΣΔ modulators, which are widely used in A/D conversion circuits, especially when high resolution is required [7]. The strength of the classical ΣΔ modulators comes from the use of oversampling and a feedback loop. The oversampling makes it possible to achieve an interesting signal-to-noise ratio (SNR), even when coding the signal with a single bit. Moreover, the feedback loop is designed to achieve three primary goals. First, to shape the power spectral density (PSD) of the quantization error (or quantization noise), minimizing its influence on the output signal in the frequency range of interest. The second goal is to ensure that the input signal appears at the converter output in the frequency range of interest. And last but not least, to ensure that the closed-loop system is stable.

In the classical ΣΔ modulators, the noise-shaping filter is electronic and fully configurable by the designer. There exist well-established methods and numerical tools, allowing for an efficient modulator design. Nevertheless, the noise-shaping filter of the EM-ΣΔ is composed of an electronic filter and a mechanical element – the sense mode –, which is not configurable. Then, while the design of the classical ΣΔ modulators is well established, the design of the electronic filter of the EM-ΣΔ modulator may be a difficult task [7]. In addition to the fixed structure of the mechanical transfer (sense mode), one of the main issues comes from the fact that this transfer is often uncertain due to fabrication dispersion, environmental variation as well as imperfect modeling. Moreover, high-frequency resonant modes may arise from the electrostatic comb fingers, adding an extra phase lag to the system, compromising its stability [6]. The inclusion of the sense mode also adds noise into the loop (due to mechanical-thermal noise, charge amplifiers, and ADC) [8]. Thus, additionally to the standard specifications (minimize the quantization error and reproduce at the output the input signal), the design of the electronic filter has three more objectives to pursue. The first one is to ensure the stability of the closed-loop system, despite the uncertainties related to the mechanical transfer, *i.e.*, robust stability. The second one is to minimize the effects of the different noises over the output signal. Finally, an additional specification can be the minimization of the displacements of the sense mode [9].

Some design methods for the electronic filter are proposed in the literature. In [1], inspired by the classical ΣΔ modulators, the authors choose a filter composed of a second-order resonator associated with a lead-phase compensator. The resonator adds zeros on the quantization noise transfer function (QNTF), whereas the compensator provides the required phase to ensure the stability of the closed-loop system. The effects of the electronic noises are evaluated afterward in [8]. In [7], the authors show that with one additional

feedback, the same design flow of the classical ΣΔ modulators can be applied for the EM-ΣΔ feedback, providing a systematic design methodology and ensuring robustness against the relay. Nevertheless, the effects of the all noise sources are not considered for the filter design, and the robust stability is only partially ensured.

More recently, the use of genetic algorithms was also proposed [5, 9]. The main advantage of this approach is that it allows choosing a multi-objective criterion to be optimized. In these works, the criterion consists of (i) minimizing the effect of the noises and quantization error on the output; and (ii) minimizing the displacements of the proof mass. The main issue of this approach, however, is that the solutions do not provide any formal guarantee of performance or robust stability.

In this work, we propose a systematic method to design the EM-ΣΔ electronic filter, guaranteeing both performance and robust stability. This method is based on the celebrated H_∞ synthesis [10], which is a very flexible design method, allowing to express and to ensure different performance specifications in the frequency domain. Indeed, these specifications are ensured by imposing prescribed shapes on the magnitude of closed-loop transfer functions. Moreover, appropriate frequency-domain constraints also guarantee the robust stability of the system. The critical point of the H_∞ design is a suitable choice of the closed-loop transfer functions and the so-called weighting filters to impose appropriate frequency constraints. Furthermore, we consider the digital implementation of the electronic filter, taking into account the sampling-and-hold effects.

The standard H_∞ design method is conceived for linear systems, which is not generally the case of the EM-ΣΔ architecture. Thus, to apply this method, we model the relay (1-bit quantizer) as an uncertain gain and a quantization error, as usually done for the EM-ΣΔ filter design [1, 6, 7]. Moreover, with our method, even the constrained nature of EM-ΣΔ filters can be treated by applying the structured H_∞ method [11], keeping the main benefits of the standard H_∞ design method.

The remaining of this paper is organized as follows. In Section 2, we revisit the EM-ΣΔ feedback, formalizing the control objectives. In Section 3, the standard H_∞ synthesis is presented. In Section 4, the H_∞ synthesis is applied to a given EM-ΣΔ architecture. The proposed method is applied to a prototype, and the results are presented in Section 5. Conclusions are drawn in Section 6.

2. EM-ΣΔ Architecture and Control Problem

In this section, we aim at describing the EM-ΣΔ architecture. Then, in a second time, we discuss the expected behavior of the closed-loop system, highlighting the main control objectives and defining the control problem.

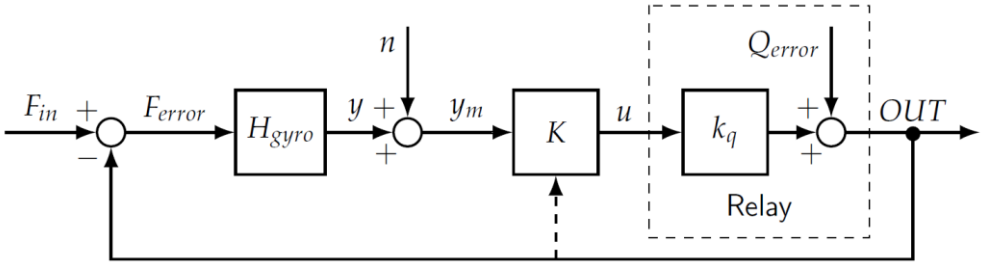

Figure 1 - General scheme of the EMΣΔ architecture

The EM-ΣΔ architecture is mainly composed of the sense mode, an electronic filter, and a relay (or 1-bit quantizer). The relay feeds back a signal that shall compensate for the disturbing forces at the input of the sense mode, as illustrated in Fig. 1. Because of its role in a feedback loop, in this work, we consider the electronic filter as a controller.

In the scheme of Figure 1, the gyroscope is represented by H_{gyro}, which models the mechanical part of the sense mode as well as the excitation and detection circuits. The signal F_{in} is an image of the forces acting on the proof mass, that is, the Coriolis and coupling forces. This "force" is to be rebalanced by the signal OUT. To quantify the performance of the system, we define the error between these signals: $F_{error} = F_{in} - OUT$.

At the output of H_{gyro}, y is an image of the displacements of the proof mass. The signal n models mechanical-thermal and electronic noises as well as any bias added by the instrumentation circuits. The measured signal is then represented by $y_m = y + n$. By adopting the quasi-linear model [1], the 1-bit quantizer (relay) is modeled by an uncertain gain k_q with a quantization error, denoted Q_{error}. This relay produces the signal OUT, which can take the values $+1$ and -1.

The controller K (electronic filter) may have one or two input signals. If the controller has only one input (y_m), it is said to be a *one-degree-of-freedom* (1DoF) controller. With two inputs (y_m and OUT), it is said to be a *two-degrees-of-freedom* (2DoF) controller. We also classify the controllers as unconstrained or constrained. Controllers are said to be *unconstrained* if they can implement any transfer function of any order. On the other hand, *constrained* controllers can only implement a bounded set of transfer functions, often with

limited order. This restriction may be originated, for instance, by the implementation resolution of the controller coefficients.

Independently of the controller choice (1DoF or 2DoF, constrained or unconstrained), we can enumerate the qualitative control objectives for the EM-ΣΔ to work correctly:

i. minimize the effects of Q_{error} on OUT;

ii. minimize the effects of the different noises and bias (signal n) on OUT;

iii. minimize the displacements of the sense mode (y);

iv. ensure that the input signal appears at the output, i.e., $OUT = F_{in}$;

v. ensure the stability of the closed-loop system against the relay nonlinear effects;

vi. ensure the stability of the closed-loop system against the uncertainties of the mechanical transfer (*e.g.*, unmodeled dynamics or environmental sensitivity).

Note that it may be impossible to achieve all these specifications fully. If we take, for instance, the specification iv. ($OUT = F_{in}$), it is clear that this equality holds only if $F_{in} = \pm 1$, which is not the case for a MEMS gyroscope. However, looking at the frequency content of both signals, it is possible to make them equal in a frequency range of interest. For MEMS gyroscopes, the resonance frequency of the drive mode, ω_d, and the required bandwidth determine this frequency range of interest: $[\omega_-; \omega_+]$, which includes ω_d. Therefore, some of the defined control objectives have to be ensured, at least in the frequency range of interest. It will be specified later when the quantified version of the required specifications is defined. Assuming it is done, we thus can state the control problem as follows.

Problem 1 (Control problem): *Given H_{gyro} and k_q, compute the controller K such that the closed-loop system of Figure 1 achieves the required specifications.*

3. H_∞ Synthesis for the EMΣΔ Architecture

The H_∞ synthesis is a flexible and powerful design method that allows posing the controller design problem as an optimization problem subject to mathematical constraints. These constraints can be used to express performance criteria as well as stability margins, providing guarantees of stability and performance for the closed-loop system. In this section, we present the main concepts of the H_∞ synthesis. For further details, we refer the interested reader to [10], for instance. Without loss of generality, we consider the controller synthesis

in continuous-time. In Sec. 4, we discuss how to transpose to discrete-time the results of this section. All the dynamical models used in the sequel are supposed to be Linear Time-Invariant and are described by (a matrix of) transfer functions.

Let us consider the general control configuration of Fig. 2a, where $\tilde{P}$ is the generalized plant, defined by the to-be-controlled system; p is the vector of exogenous inputs of the system (such as the Coriolis force and noise); q is the vector of controlled outputs (*e.g.*, the estimation error or the signal OUT); and u_P and y_P are respectively the control signals (u in Fig. 1) and sensed outputs (y_m or $[y_m, OUT]^T$ of Fig. 1 for 1DoF or 2DoF controller, respectively). Moreover, weights W_{in} and W_{out} can be attributed to the different signals of interest through the so-called weighting filters (or weighting functions), as illustrated in Fig. 2b. These weighting filters are usually diagonal and define the weighted input and output vectors $w = W_{in}^{-1}p$ and $z = W_{out}q$, respectively. Therefore, the objective is to design a controller K that ensures a certain performance level $\gamma > 0$ and the stability of $T_{w\to z}$, where we use the notation $T_{a\to b}$ to represent the transfer from a signal a to a signal b. The performance level γ is defined as an upper bound on the H_∞ norm of $T_{w\to z}$, that is,

$$\|T_{w\to z}(s)\|_\infty < \gamma. \tag{1}$$

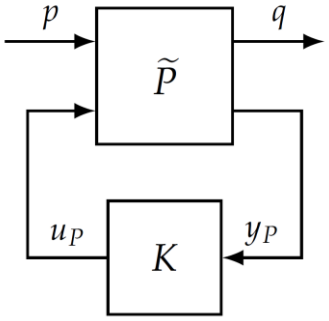

Figure 2a - General control configuration

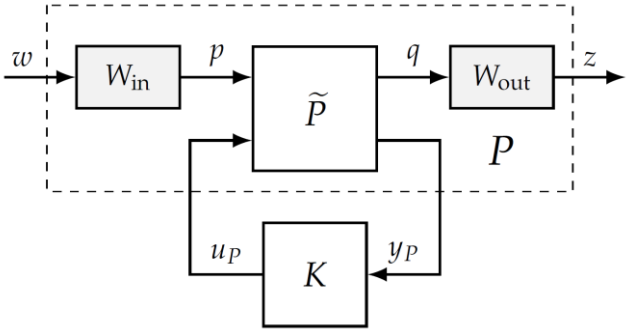

Figure 2b - General control configuration with weighting filters

Note that $T_{w\to z}(s) = W_{out}(s)T_{p\to q}(s)W_{in}(s)$ defines the so-called H_∞ criterion of (1). This criterion is defined through the choice of the signals of interest that compose the vectors p and q, as well as the weighting filters W_{in} and W_{out}.

The choice of the H_∞ criterion is one of the crucial points of the H_∞ synthesis. Indeed, the proper choice of the input and output signals and the design of the weighting functions can enforce the desired specifications and provide formal guarantees of robust stability and performance. Another crucial point is how to compute a controller that ensures the H_∞ criterion for a given performance level γ.

In the sequel of this section, we propose an H_∞ criterion adapted to the EM-ΣΔ feedback. Then, we discuss the computation of the controller for the EM-ΣΔ architecture. Two cases are considered: the unconstrained controller and the constrained one.

3.2. An H_∞ criterion for the EM-ΣΔ architecture

The first step to define the H_∞ criterion related to the EM-ΣΔ architecture (see Fig. 1) is to choose the signals of interest and compute the closed-loop transfer functions. Then, the control specifications are formulated as closed-loop frequency constraints that express the desired closed-loop behavior. Finally, weighting functions are designed to enforce these frequency constraints. Here, we consider the general case with a 2DoF controller, defined as $K = [K_1, K_2]$. For the 1DoF controller, consider the following results with $K_2 = 0$.

We start by selecting as signals of interest the inputs F_{in}, n and Q_{error}, and the outputs F_{error}, y, u and OUT. They define the input vector $p = [F_{in},\ n,\ Q_{error}]^T$ and the output vector $q = [F_{error},\ y,\ u,\ OUT]^T$. Thus, the closed-loop transfer matrix $T_{p\to q}$ is given by

$$\begin{pmatrix} T_{F_{in}\to F_{error}} & T_{n\to F_{error}} & T_{Q_{error}\to F_{error}} \\ T_{F_{in}\to y} & T_{n\to y} & T_{Q_{error}\to y} \\ T_{F_{in}\to u} & T_{n\to u} & T_{Q_{error}\to u} \\ T_{F_{in}\to OUT} & T_{n\to OUT} & T_{Q_{error}\to OUT} \end{pmatrix} = \begin{pmatrix} (1-k_qK_2)S_1 & -k_qK_1S_1 & -S_1 \\ H_{gyro}(1-k_qK_2)S_1 & -H_{gyro}k_qK_1S_1 & -H_{gyro}S_1 \\ H_{gyro}K_1S_1 & K_1S_1 & T_1/k_q \\ H_{gyro}k_qK_1S_1 & k_qK_1S_1 & S_1 \end{pmatrix}, \quad (2)$$

where $S_1 = \left(1 + k_q\left(H_{gyro}K_1 - K_2\right)\right)^{-1}$ and $T_1 = 1 - S_1$.

Remark 1: The transfer $T_{Q_{error}\to OUT} = S_1$ corresponds to the so-called (quantization) noise transfer function (NTF), the transfer $T_{n\to OUT} = k_qK_1S_1$ corresponds to the electrical/electronic noise transfer function (ENTF), and $T_{F_{in}\to OUT}$ is the signal transfer function (STF) [7,8].

Remark 2: The classical approach for designing the electronic filter (controller) consists in minimizing the NTF in the frequency range of interest [1, 7], *i.e.*,

$$\forall \omega \in [\omega_-; \omega_+],\ \left|T_{Q_{error}\to OUT}(j\omega)\right| \ll 1, \quad (3)$$

minimizing the power spectral density of the quantization noise in this frequency range.

Note that $\left|T_{Q_{error}\to F_{error}}(j\omega)\right| = \left|T_{Q_{error}\to OUT}(j\omega)\right|$. In the case of $K_2 = 0$ (1DoF), $\left|T_{Q_{error}\to F_{error}}(j\omega)\right| = \left|T_{F_{in}\to F_{error}}(j\omega)\right|$. Moreover, structurally,

$$T_{F_{in}\to F_{error}}(s) + T_{F_{in}\to OUT}(s) = 1. \quad (4)$$

Then, (3) implies that the STF $\left|T_{F_{in}\to OUT}(j\omega)\right| \approx 1$ for all $\omega \in [\omega_-; \omega_+]$. Nevertheless, if $K_2 \neq 0$ (2DoF), except for some particular cases, $\left|T_{Q_{error}\to F_{error}}(j\omega)\right| \neq \left|T_{F_{in}\to F_{error}}(j\omega)\right|$.

Hence, designing an adequate NTF does not automatically imply that the STF is adequate for the application.

Remark 3: A similar reasoning is applied for the transfers to y. In the case of $K_2 = 0$ (1DoF), when (3) is ensured, $|T_{F_{in}\to y}(j\omega)| = |T_{Q_{error}\to y}(j\omega)| \approx 1/|K_1(j\omega)|$. Since $|K_1(j\omega)|$ is usually high in the range $[\omega_-;\omega_+]$ (to ensure (3)), it minimizes the displacements of the proof mass in this frequency range. Now, if $K_2 \neq 0$ (2DoF), and except for particular cases, the displacements of the proof mass are not necessarily minimized, even if (3) is satisfied.

Let us now translate the control specifications of Sec. 2 into mathematical constraints on the closed-loop frequency responses, as follows.

- *Minimization of the effects of Q_{error} and n on OUT:* minimizing the effects of the quantization error and different noises n on the signal OUT corresponds to impose,

$$\forall\omega \in [\omega_-;\omega_+], \quad |T_{Q_{error}\to OUT}(j\omega)| \ll 1 \text{ and } |T_{n\to OUT}(j\omega)| \ll 1. \tag{5}$$

  Since $|T_{Q_{error}\to OUT}(j\omega)| = |T_{Q_{error}\to F_{error}}(j\omega)|$ and $|T_{n\to OUT}(j\omega)| = |T_{n\to F_{error}}(j\omega)|$, the above conditions are equivalent to

$$\forall\omega \in [\omega_-;\omega_+], \quad |T_{Q_{error}\to F_{error}}(j\omega)| \ll 1 \text{ and } |T_{n\to F_{error}}(j\omega)| \ll 1. \tag{6}$$

- *Ensure that OUT tracks the input signal F_{in}:* to have $OUT = F_{in}$, the transfer $T_{F_{in}\to OUT}$ must be equal to one. Note that $T_{F_{in}\to F_{error}} + T_{F_{in}\to OUT} = 1$. Then, with

$$\forall\omega \approx \omega_x, \quad |T_{F_{in}\to F_{error}}(j\omega)| \ll 1, \tag{7}$$

  we ensure $OUT \approx F_{in}$, at least for the frequency range of interest $[\omega_-;\omega_+]$.

- *Displacements minimization:* this specification corresponds to minimizing the magnitude of the transfers $T_{F_{in}\to y}$, $T_{n\to y}$, $T_{Q_{error}\to y}$ not only for $[\omega_-;\omega_+]$ bur for all frequencies, that is,

$$\forall\omega, \quad |T_{F_{in}\to y}(j\omega)| \leq k_1, \quad |T_{n\to y}(j\omega)| \leq k_2 \quad \text{and} \quad |T_{Q_{error}\to y}(j\omega)| \leq k_3, \tag{8}$$

  where k_1, k_2 and k_3 are constant parameters defined by the designer.

- *Robustness against the relay:* for the controller design, the quasi-linear model of the relay is adopted, *i.e.*, the relay is modeled as an uncertain gain with additive noise, as in [1, 7]. Then, to make the closed-loop system robust against this uncertain gain, the condition

$$\|T_{Q_{error}\to OUT}\|_\infty < 2 \tag{8}$$

is generally considered for stability [7]. Because $T_{Q_{error}\to OUT} = S_1$, which represents a sensitivity function from the Control Theory point of view [10], this condition corresponds to a modulus margin at the output or input of the relay $\Delta M_1 > 0.5$, implying sufficient phase and gain margins (against the uncertain gain k_q). Strictly speaking, this condition is valid only for the quasi-linear model; it does not mathematically apply for the nonlinear system, with the real relay. However, in the absence of a simple formal stability measure, this condition has been used in practice [7]. In light of this discussion, it is also essential to keep the relay operating as close as possible to a "linear" behavior, avoiding saturation of the quantizer (see Sec. 5). To this purpose, the bias at the relay input (signal u) has to be minimized as well as its high-frequency components. That is,

$$\forall \omega \approx 0, \quad \left|T_{F_{in}\to u}(j\omega)\right| \ll 1, \quad |T_{n\to u}(j\omega)| \ll 1 \quad \text{and} \quad \left|T_{Q_{error}\to u}(j\omega)\right| \ll 1 \tag{9}$$

$$\forall \omega \gg \omega_+, \quad \left|T_{F_{in}\to u}(j\omega)\right| \ll 1, \ |T_{n\to u}(j\omega)| \ll 1 \ \text{and} \ \left|T_{Q_{error}\to u}(j\omega)\right| \ll 1. \tag{10}$$

- *Robustness against the model uncertainties:* a typical choice to enforce good stability margins against model uncertainties is to choose a convenient modulus margin at the input or output of the gyroscope model H_{gyro} [10]. In this case, the sensitivity function is given by $S_2 = T_{F_{in}\to F_{error}}$. Then, the modulus margin is given by $\Delta M_2 = 1/\|S_2\|_\infty$. So, by restricting the maximum value of $|S_2|$, a minimum modulus margin can be enforced.

  Further than the modulus margin ΔM_2, additive and multiplicative uncertainties can be considered to take into account the high-frequency resonant modes of the comb fingers. By bounding $\left|T_{n\to F_{error}}\right|$ and $\left|T_{n\to y}\right|$ in the frequency range where the high-frequency resonant modes are located, the robust stability of the closed-loop system against those high-frequency modes can be ensured [10].

Please note that the closed-loop specifications are frequency-dependent. To take into account this dependency, we add weighting filters on the signals of interest, as presented in the H_∞ criterion of Fig. 3. Notice that hereafter the signal OUT is not taken into account. The output vector is henceforth given by $q = [F_{error},\ y,\ u]^T$. This follows from the fact that there are no constraints on $T_{F_{in}\to OUT}$ (to have $OUT = F_{in}$, the constraints are on $T_{F_{in}\to F_{error}}$ instead) and from the redundancies in (2): $|T_{n\to OUT}| = \left|T_{n\to F_{error}}\right|$ and $\left|T_{Q_{error}\to OUT}\right| = \left|T_{Q_{error}\to F_{error}}\right|$.

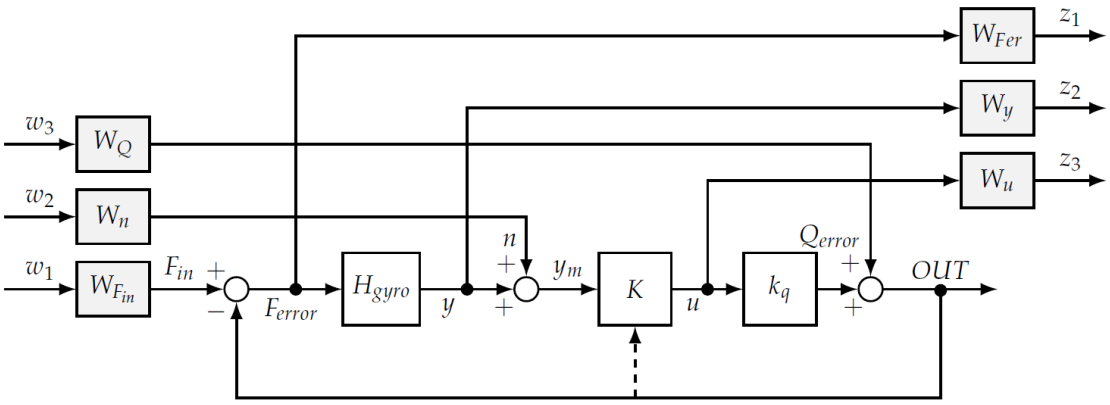

Figure 3 - H_∞ criterion for the EM-ΣΔ architecture

Therefore, the general H_∞ EM-ΣΔ design problem can be stated as follows.

Problem 2 (General H_∞-based EM-ΣΔ design problem): *Given a generalized plant P (which is defined by H_{gyro}, k_q and the weighting functions) and a performance level $\gamma > 0$, compute a controller $K \in \mathcal{K}$ that stabilizes $T_{w\to z}$ and ensures $\|T_{w\to z}\|_\infty < \gamma$.*

The set $\mathcal{K}$ of controllers is defined in sections 3.3 and 3.4, depending on their structure. However, regardless of the controller structure, if the optimization problem above has a solution, the following inequality holds

$$\left\| \begin{pmatrix} W_{Fer} & 0 & 0 \\ 0 & W_y & 0 \\ 0 & 0 & W_u \end{pmatrix} \begin{pmatrix} T_{F_{in}\to F_{error}} & T_{n\to F_{error}} & T_{Q_{error}\to F_{error}} \\ T_{F_{in}\to y} & T_{n\to y} & T_{Q_{error}\to y} \\ T_{F_{in}\to u} & T_{n\to u} & T_{Q_{error}\to u} \end{pmatrix} \begin{pmatrix} W_{Fin} & 0 & 0 \\ 0 & W_n & 0 \\ 0 & 0 & W_Q \end{pmatrix} \right\|_\infty < \gamma. \quad (11)$$

Moreover, $\forall\ \omega \in \mathbb{R}$, (11) implies (where frequency dependence $(j\omega)$ is omitted):

$$|T_{F_{in}\to F_{error}}| < \frac{\gamma}{|W_{Fer}\cdot W_{Fin}|}, \quad |T_{n\to F_{error}}| < \frac{\gamma}{|W_{Fer}\cdot W_n|}, \quad |T_{Q\to F_{error}}| < \frac{\gamma}{|W_{Fer}\cdot W_Q|},$$

$$|T_{F_{in}\to y}| < \frac{\gamma}{|W_y\cdot W_{Fin}|}, \quad |T_{n\to y}| < \frac{\gamma}{|W_y\cdot W_n|}, \quad |T_{Q\to y}| < \frac{\gamma}{|W_y\cdot W_Q|},$$

$$|T_{F_{in}\to u}| < \frac{\gamma}{|W_u\cdot W_{Fin}|}, \quad |T_{n\to y}| < \frac{\gamma}{|W_u\cdot W_n|}, \quad |T_{Q\to y}| < \frac{\gamma}{|W_u\cdot W_Q|}.$$

Note that if $\gamma \leq 1$, the weighting functions define an upper bound on the magnitude of the closed-loop transfer functions. Then, the proper choice of the weighting functions allows one to express and ensure the closed-loop constraints and, hence, the control specifications.

We emphasize that the H_∞ criterion here presented can be employed to any EM-ΣΔ architecture in the form of Fig. 1, regardless of the controller structure (constrained or unconstrained). The structure of the controller determines the optimization method that is used to solve Problem 2. This point is discussed in the sequel.

3.3. A solution to the unconstrained case

An EMΣΔ controller is said to be unconstrained if it admits a state-space representation of the form

$$K: \begin{cases} \dot{x}_K(t) = A_K x_K(t) + B_K y_P(t) \\ u_P(t) = C_K x_K(t) + D_K y_P(t) \end{cases}, \tag{12}$$

where $x_K(t) \in \mathbb{R}^{n_K}$ with $n_K = n_P$ and n_P being the order of H_{gyro} plus the total order of all the weighting function\ns. The state-space matrices are real-valued and have adequate dimensions. They define any transfer function $K(s)$ of order n_K with n_{y_P} inputs and n_{u_P} outputs. That is, for the unconstrained case, the set $\mathcal{K}$ is defined as $\mathcal{K} = \mathcal{R}_p^{n_{y_P} \times n_{u_P}}$, where $\mathcal{R}_p^{n_{y_P} \times n_{u_P}}$ is the set of all rational proper transfer matrices of dimension $n_{y_P} \times n_{u_P}$.

For the case of an unconstrained controller, Problem 2 is a convex optimization problem and can therefore be solved efficiently, *i.e.*, in a reasonable time [11]. The main advantage of dealing with convex optimization problems is that if there exists a solution to the problem, the solution is always found. The problem is that, in general, the EM-ΣΔ controllers are constrained.

3.4. A solution to the constrained case

In most of the EM-ΣΔ feedbacks, the controller structure is constrained. That is, the controller does not admit the general state-space representation of (12). This limitation can have some origins, such as (i) the order of the controller is less than n_K; or (ii) implementation constraints, as a limitation of the gains, for instance.

In this framework, we tackle the controller design as a static output feedback problem with the configuration of Figs. 2a and 2b, where the predefined dynamics (integrators) of the controller are encapsulated into a new $\tilde{P}$, such that $u_P = K y_P$. In this case, $\mathcal{K}$ is a subset of real matrices. This subset is defined by the structure of the controller and implementation constraints. Therefore, Problem 2 becomes an H_∞ synthesis problem with structural constraints [11]. In this case, the optimization problem is no longer convex. Then, the solution may depend on the initial point and, even if there exists a solution to the problem, there are no guarantees that this solution will be found. However, with good initialization, this problem can be tackled by efficient optimization methods [11].

The difficulty here is how to define the subset $\mathcal{K}$ and the new generalized plant $\tilde{P}$. This subject is discussed in the next section.

4. H_∞ Synthesis for a Constrained EM-ΣΔ Controller

In this section, we apply the proposed method to design the controller parameters of a particular EM-ΣΔ architecture. Nevertheless, we emphasize that the procedure here applied can be extended to other EM-ΣΔ architectures.

We consider the architecture detailed in Fig. 4, which is similar to the one proposed in [4], and where the digital elements work with a sampling time $T_s = \frac{2\pi}{36\omega_d}$. We use a MEMS gyroscope from Tronic's Microsystems (GYPRO family), whose dynamic behavior (including actuation and instrumentation circuits) is modeled by

$$H_{gyro}(s) = \frac{k_0\omega_s^2}{s^2+s\cdot\omega_s/Q_s+\omega_s^2}, \tag{13}$$

where $k_0 = 0.0759$ is the static gain, $\omega_s = 1.004 \cdot \omega_d$ is the resonance frequency and $Q_s = 23.4 \cdot 10^3$ is the quality factor of the sense mode. For the controller synthesis, we adopt $k_q = 1$.

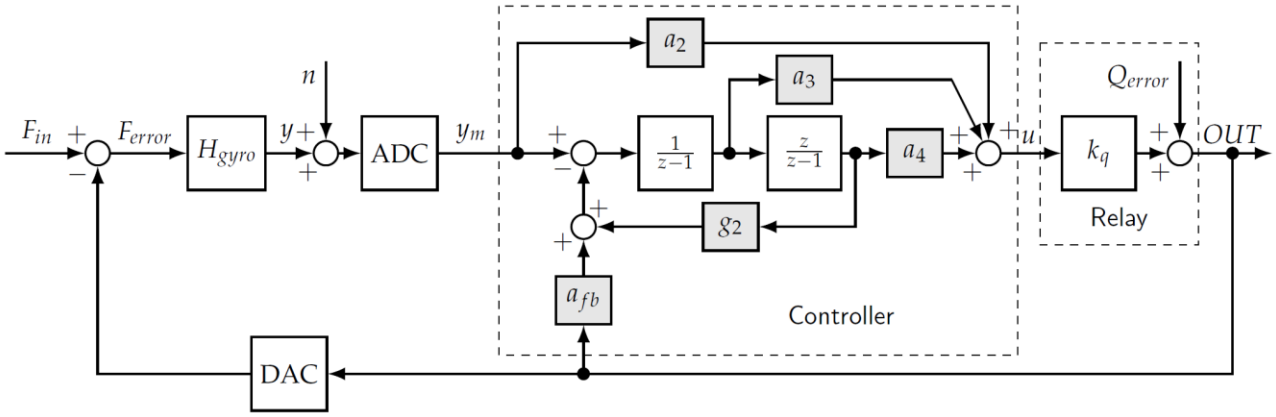

Figure 4. EM-ΣΔ architecture. In gray, we represent the electronic filter coefficients to be designed

Some facts justify the fact that this controller is constrained. First, it has only two integrators, *i.e.*, $n_K = 2$. If any of the weighting functions of the H_∞ criterion has an order greater than zero, the order of the generalized plant is greater than 2. Moreover, due to the predefined structure of the controller, its poles and zeros cannot be placed arbitrarily. For instance, this structure fixes the z-domain poles p_{z1} and p_{z2} such that $p_{z1} \cdot p_{z2} = 1$, constraining the set of possible controllers.

The objective is to compute the parameters a_2, a_3, a_4, a_{fb} and g_2 such that the closed-loop system is stable and verifies the specifications of Sec. 2. Thus, we apply the following steps:

i. the first step is to discretize H_{gyro}, taking the sampling-and-holding effects into account;

ii. then, a generalized plant $\tilde{P}$ is defined, including H_{gyro} and the dynamics of the controller (integrators), and the subset $\mathcal{K}$ is also defined;

iii. the weighting functions are designed to enforce the desired specifications; and

iv. finally, the controller is computed by solving Problem 2 with the subset $\mathcal{K}$ defined in step ii.

4.1. Discretization of H_{gyro}

The first step to designing the controller, which is implemented in discrete-time, is to obtain an equivalent discrete-time model of H_{gyro}. Moreover, this model has to take into consideration the effects of sampling-and-holding (ADC and DAC). To this purpose, we apply the step-invariant method [12], obtaining

$$H_{gyro}^{ZOH}(z) = (1 - \mathrm{z}^{-1})\mathcal{Z}\left\{\mathcal{L}^{-1}\left\{\frac{H_{gyro}(s)}{\mathrm{s}}\right\}\right\}, \tag{15}$$

where $\mathcal{Z}$ is the z-transform and $\mathcal{L}^{-1}$ is the inverse Laplace transform.

4.2. Defining the generalized plant $\tilde{P}$ and the subset $\mathcal{K}$

The next step is to define the generalized plant $\tilde{P}$ and the subset $\mathcal{K}$. To this purpose, we isolate the to-be-designed parameters from the rest of the system, defining $\tilde{P}$, as illustrated in Fig. 5. The signals entering the to-be-designed parameters define the sensed signal vector $y_P = [y_1, y_2, y_3, y_4]^T$. The signals delivered by these parameters define the control signal vector $u_P = [u_1, u_2]^T$.

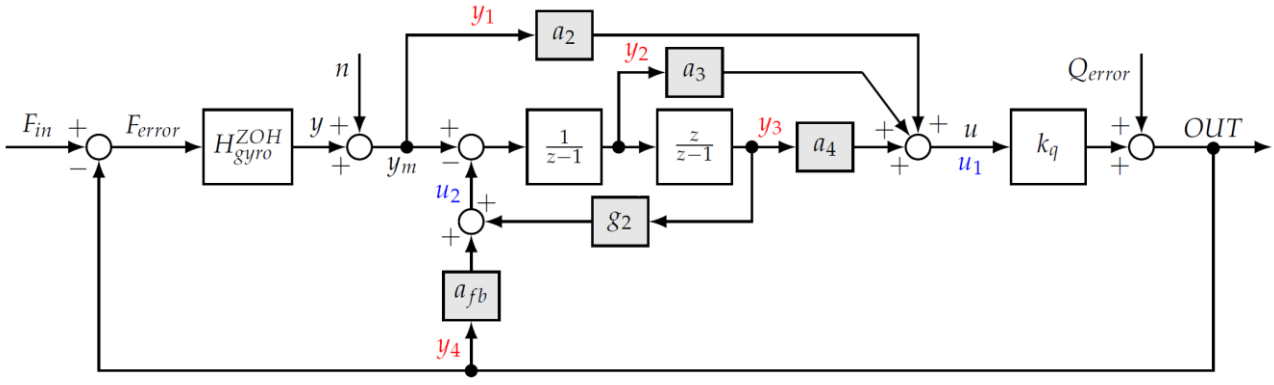

Figure 5. EM-ΣΔ architecture. In gray, we represent the electronic filter coefficients to be designed; in blue, the signals composing u_P; and in red, the signals defining y_P

Note that $u_P = \begin{pmatrix} a_2 & a_3 & a_4 & 0 \\ 0 & 0 & g_2 & a_{fb} \end{pmatrix} y_P$, defining the subset $\mathcal{K}$ as

$$\mathcal{K} = \left\{ \begin{array}{c} K \mid \exists\, a_2 \in \left[\underline{a_2},\ \overline{a_2}\right], \exists\, a_3 \in \left[\underline{a_3}, \overline{a_3}\right], \exists\, a_4 \in \left[\underline{a_4}, \overline{a_4}\right], \\ \exists\, g_2 \in \left[\underline{g_2}, \overline{g_2}\right], \exists\, a_{fb} \in \left[\underline{a_{fb}}, \overline{a_{fb}}\right], \\ K = \begin{pmatrix} a_2 & a_3 & a_4 & 0 \\ 0 & 0 & g_2 & a_{fb} \end{pmatrix} \end{array} \right\}. \quad (15)$$

The notation $\overline{(\cdot)}$ and $\underline{(\cdot)}$ indicates the upper and lower bounds of $(\cdot)$, respectively.

Finally, $\tilde{P}$ is defined as the transfer that maps the inputs $p = [F_{in},\ n,\ Q_{error}]^T$ and u_P into the outputs $q = [F_{error}, y, u]^T$ and y_P.

Note that the generalized plant $\tilde{P}$ is in discrete-time. Although it is possible to make the design in discrete-time, for frequency-domain design methods (as the H_∞ synthesis), it is more convenient to use equivalent continuous-time models. The main reason is that in continuous-time, conventional frequency-domain techniques can be used. The equivalent continuous-time model is obtained through the bilinear (or Tustin) transform of $\tilde{P}$ [12].

4.3. Weighting functions and controller design

The weighting functions, thanks to (11), define upper bounds on $T_{p\to q}$ and, therefore, enforce the performance specifications of Sec. 3.2. The controller constraints are also taken into account. Hence, we design the continuous-time weighting functions such that the frequency constraints correspond to the upper bounds presented in Figs. 6 and 7. The latter one presents a zoom around ω_d (the resonance frequency of the drive mode), which normalizes the frequency axis. The proposed method is applied, obtaining closed-loop transfers whose frequency responses are identified as CL_new. For the sake of comparison, we also present the frequency responses obtained with an established set of parameters. These transfers are identified as CL_old.

Please note that, globally, CL_old and CL_new have similar frequency responses around ω_d (normalized frequency equal to 1) and for higher frequencies. The main difference appears in low frequencies. This behavior is justified by the choice of the weighting functions (upper bounds), which, to ensure that the relay operates “linearly” (see constraint of (9)), enforce the transfers to u (the relay input) to have low gains in low frequencies, reducing the offset at the relay input. Moreover, we obtain $\left\|T_{Q_{error}\to F_{error}}\right\|_\infty < 1.3$, ensuring good stability margins against the uncertain gain k_q. We also obtain $\|S_2\|_\infty = \left\|T_{F_{in}\to F_{error}}\right\|_\infty < 4.4$, providing an adequate stability margin with respect to the model uncertainties. Because of the controller constraints, this value cannot be reduced further with the constraint of (5).

Note that the upper bound on $\left|T_{Q_{error}\to F_{error}}\right|$ shapes the NTF such that the quantification error on the signal OUT is minimized around ω_d. Also note that the proposed approach allows reducing the effects of the noises n on OUT (equivalent to $T_{n\to F_{error}}$). Due to controller constraints (structural constraints), the transfers $T_{F_{in}\to F_{error}}$, $T_{F_{in}\to y}$, $T_{n\to F_{error}}$ and $T_{n\to y}$ cannot be minimized around ω_d. Still, the proposed approach allows optimizing the global behavior of the closed-loop system, at least on the transfers and frequency ranges in which the controller structure allows so.

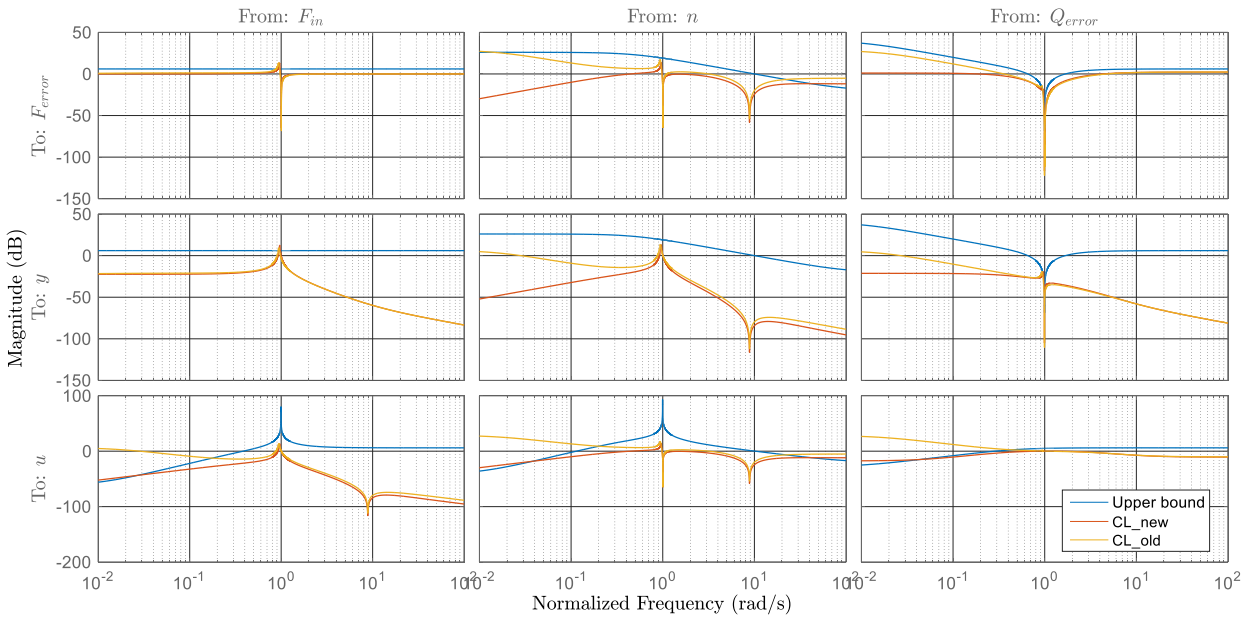

Figure 6. Closed-loop transfer functions

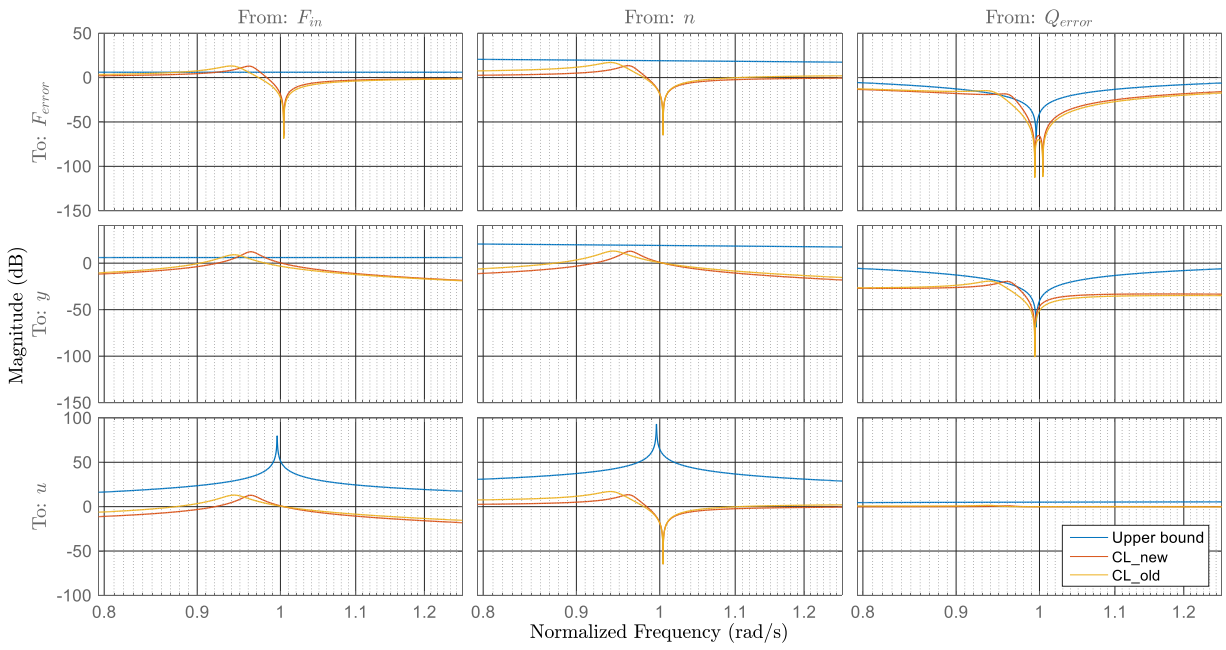

Figure 7. Closed-loop transfer functions. Zoom around the resonance frequency ω_d

5. Implementation Results

In this section, we present the implementation results obtained with the proposed approach, always comparing with the performance obtained with CL_old.

First, we measure the signal OUT with the two different sets of parameters (CL_old and CL_new) with the gyroscope at rest and with the drive mode operating normally. The results are presented in Fig. 8. Please note that with CL_old, the relay output seems to be saturated. Then, the quasi-linear model of the relay cannot be considered for this set of parameters. Indeed, when the output stays in 1, the closed-loop system behaves as if it was in open-loop operation. On the other hand, with CL_new, the signal OUT is more equilibrated (with an average close to zero). This improvement is achieved through the attenuation of the offset (or low-frequency) signals on u. When comparing the power spectral density (PSD) of OUT for the two sets of parameters – see Figs. 9 and 10 –, we can note a substantial reduction of the low-frequency components (up to 70 dB attenuation). The noise level is also reduced in almost all the frequency range, especially around ω_d. The peak that appears at $\omega = 1$ corresponds to the coupling force, which transfers part of the oscillations from the drive mode to the sense one (parasitic mechanical coupling).

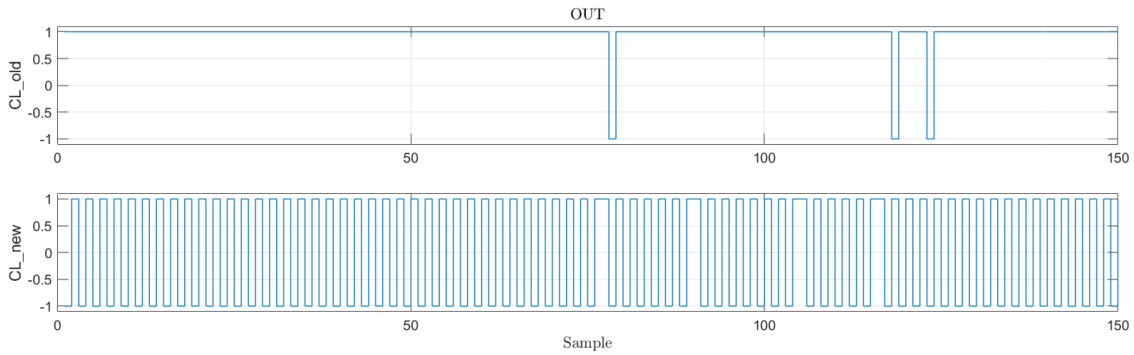

Figure 8. Measures of the signal OUT for the two approaches

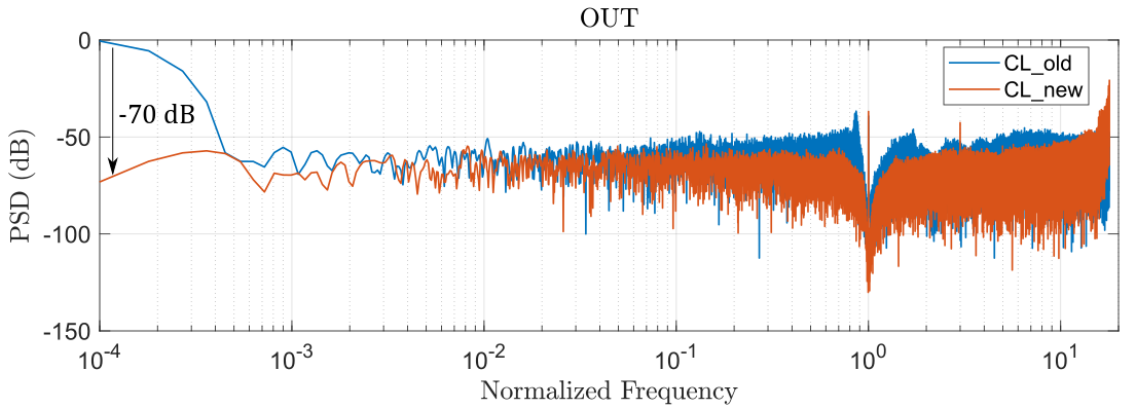

Figure 9. PSD of the measures of the signal OUT for the two approaches

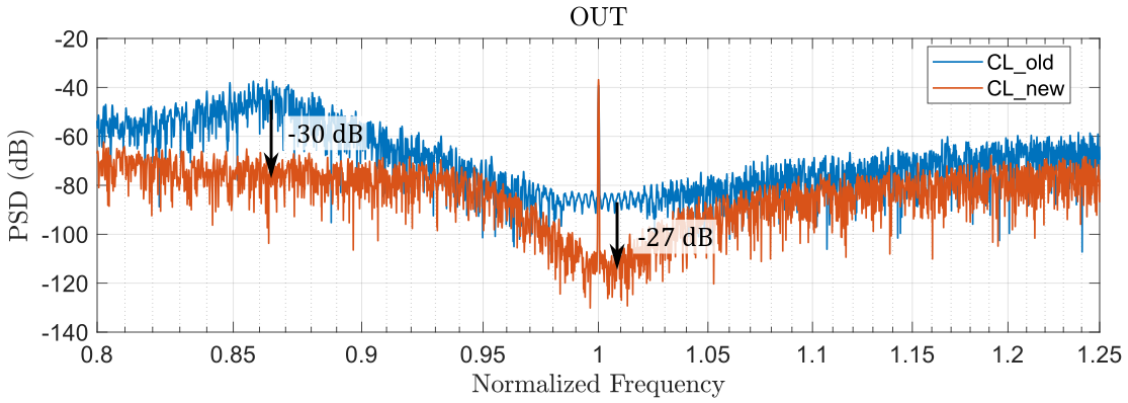

Figure 10. PSD of the measures of the signal OUT for the two approaches. Zoom around ω_d

The same approach with the similar frequency constraints is applied to six different gyroscopes of the same family, and characterization tests are performed. The average results are presented in Table 1, where we can observe a significant improvement of more than 30% on the scale factor nonlinearity (SFNL), the RMS noise, and the angle-random walk (ARW). These parameters are mainly linked to the linear behavior of the sensor (SFNL) and the noise on the signal OUT. As discussed earlier, these aspects are greatly enhanced with CL_new. Moreover, although the (more) modest performance improvement on scale factor over temperature (SFOT) and bias over temperature (BOT), our approach demonstrates to be as robust as the established one for temperature changes. Regarding the bias instability (BI), the performance of both approaches are similar.

Table 1 – Results for a set of six gyroscopes

Parameter	SFNL (ppm)	RMS noise $(°/s)$	ARW $(°/\sqrt{h})$	BI $(°/h)$	SFOT (%)	BOT $(°/s)$
CL_old	259	0.035	0.148	0.317	0.032	0.013
CL_new	150	0.020	0.097	0.302	0.029	0.010
Improvement	32%	43%	34%	5%	10%	22%

6. Conclusion

In this work, a new method for designing the electronic filter of an EM-ΣΔ feedback was presented. This approach is based on the H_∞ synthesis, which is a flexible and systematic control design method. The choice of an adequate H_∞ criterion is one of the crucial points of the H_∞ synthesis. In this paper, we propose an H_∞ criterion that is suited for any EM-ΣΔ architecture, regardless of the controller structure. The desired specifications are expressed through the weighting functions, which can be adapted by the designer. Another crucial point is the computation of the controller. Here, two cases appear: the unconstrained and the

constrained cases. We focus on the latter one, which represents most of the controllers in EM-ΣΔ feedbacks.

To illustrate the use of our method, we consider a given EM-ΣΔ architecture. A new electronic filter is designed and compared to an established one. The flexibility of our method allows us to better manage the nonlinearities of the relay, despite the controller constraints, reflecting in an improvement of the sensor performance parameters.

Future works are focused on the inclusion of other parameters in the design method, such as the gains of the charge amplifiers. Moreover, tests with a more extensive set of gyroscopes are also planned.

References

[1] V. P. Petkov and B. E. Boser, “A fourth-order SigmaDelta interface for micromachined inertial sensors,” *IEEE J. Solid-State Circuits*, vol. 40, no. 8, pp. 1602–1609, Aug. 2005.

[2] A. K. El-Shennawy, H. Aboushady, and A. El-Sayed, “Design method for a ΣΔ-based closed loop gyroscope,” *Int. Des. Test Work.*, 2009.

[3] J. Raman, E. Cretu, P. Rombouts, and L. Weyten, “A Closed-Loop Digitally Controlled MEMS Gyroscope With Unconstrained Sigma-Delta Force-Feedback,” *IEEE Sens. J.*, vol. 9, no. 3, pp. 297–305, Mar. 2009.

[4] A. Elsayed *et al.*, “A self-clocked ASIC interface for MEMS gyroscope with 1m noise floor,” in *IEEE Custom Integrated Circuits Conference*, 2011.

[5] F. Chen, W. Yuan, H. Chang, G. Yuan, J. Xie, and M. Kraft, “Design and Implementation of an Optimized Double Closed-Loop Control System for MEMS Vibratory Gyroscope,” *IEEE Sens. J.*, vol. 14, no. 1, pp. 184–196, Jan. 2014.

[6] F. Chen, X. Li, and M. Kraft, “Electro-mechanical Sigma-Delta Modulators (ΣΔM) Force Feedback Interfaces for Capacitive MEMS Inertial Sensors: A Review,” *IEEE Sens. J.*, vol. 16, no. 17, pp. 6476–6495, 2016.

[7] J. Raman, P. Rombouts, and L. Weyten, “An Unconstrained Architecture for Systematic Design of Higher Order ΣΔ Force-Feedback Loops,” *IEEE Trans. Circuits Syst. I Regul. Pap.*, vol. 55, no. 6, pp. 1601–1614, Jul. 2008.

[8] V. P. Petkov and B. E. Boser, “High-order electro-mechanical Sigma-Delta modulation in micromachined inertial sensors,” *IEEE Trans. Circuits Syst. I Regul. Pap.*, vol. 53, no. 5, pp. 1016–1022, May 2006.

[9] R. Wilcock and M. Kraft, “Genetic algorithm for the design of electro-mechanical sigma delta modulator MEMS sensors,” *Sensors*, vol. 11, no. 10, pp. 9217–9232, 2011.

[10] S. Skogestad and I. Postlethwaite, Multivariable Feedback Control - Analysis and design, 2nd edition. John Wiley & Sons, 2001.

[11] P. Apkarian and D. Noll, “Nonsmooth H_∞ Synthesis,” IEEE Trans. Automat. Contr., 2006.

[12] K. J. Åström and B. Wittenmark, *Computer-Controlled Systems Theory and Design*, Third Edition. Prentice Hall, 2013.